Marine Pollution Bulletin 177 (2022) 113487

Contents lists available at ScienceDirect

Marine Pollution Bulletin

journal homepage: www.elsevier.com/locate/marpolbul

Ex vivo exposure to titanium dioxide and silver nanoparticles mildly affect sperm of gilthead seabream (*Sparus aurata*) - A multiparameter spermiotoxicity approach

A. Carvalhais [a], I.B. Oliveira [b,*], H. Oliveira [a], C.C.V. Oliveira [c], L. Ferrão [c,d], E. Cabrita [c], J. F. Asturiano [d], S. Guilherme [a], M. Pacheco [a], C.L. Mieiro [a]

[a] CESAM and Department of Biology, University of Aveiro, Campus Universitário de Santiago, 3810-193 Aveiro, Portugal
[b] Interdisciplinary Centre of Marine and Environmental Research (CIIMAR), University of Porto, 4450-208 Matosinhos, Portugal
[c] Centre of Marine Sciences (CCMAR), University of Algarve, Campus de Gambelas, 8005-139 Faro, Portugal
[d] Grupo de Acuicultura y Biodiversidad, Instituto de Ciencia y Tecnología Animal, Universitat Politècnica de València, Spain

ARTICLE INFO

Keywords:
Reprotoxicity
Gametes
Marine fish
Short-term exposure
Sub-lethal effects
Quiescent sperm

ABSTRACT

Nanoparticles (NP) are potentially reprotoxic, which may compromise the success of populations. However, the reprotoxicity of NP is still scarcely addressed in marine fish. Therefore, we evaluated the impacts of environmentally relevant and supra environmental concentrations of titanium dioxide (TiO_2: 10 to 10,000 $\mu g \cdot L^{-1}$) and silver NP (Ag: 0.25 to 250 $\mu g \cdot L^{-1}$) on the sperm of gilthead seabream (*Sparus aurata*). We performed short-term direct exposures (*ex vivo*) and evaluated sperm motility, head morphometry, mitochondrial function, antioxidant responses and DNA integrity. No alteration in sperm motility (except for supra environmental Ag NP concentration), head morphometry, mitochondrial function, and DNA integrity occurred. However, depletion of all antioxidants occurred after exposure to TiO_2 NP, whereas SOD decreased after exposure to Ag NP (lowest and intermediate concentration). Considering our results, the decrease in antioxidants did not indicate vulnerability towards oxidative stress. TiO_2 NP and Ag NP induced low spermiotoxicity, without proven relevant ecological impacts.

1. Introduction

The unique physicochemical properties of nanoparticles (NP) are attractive to industry, medicine and consumer products, leading to their massive production and widespread dispersal into the environment, namely into the marine ecosystems as the ultimate destination of contaminants (Kurwadkar et al., 2015; Shaalan et al., 2016). Titanium dioxide NP (TiO_2 NP) and silver NP (Ag NP) are used in a broad range of products, including sunscreens, cosmetics, dyes, antimicrobial products, whose production corresponds to 89–97% of the total NP emissions into the environment. These NP are considered the most relevant concerning human and environmental hazards (Keller et al., 2013).

The available information on the toxicity of NP points towards oxidative stress, cyto- and genotoxicity, changes in immunological alterations and histopathological lesions (Auguste et al., 2019; Barmo et al., 2013; Canesi et al., 2010; Magesky and Pelletier, 2018; Mieiro et al., 2019; Vignardi et al., 2015). However, limited data exist regarding their toxic potential in reproduction (reprotoxicity). The available studies on male nanoreprotoxicity mainly focused on mammals and suggest that NP induce testicular toxicity through hormonal imbalance and oxidative stress, which negatively affects sperm DNA integrity, the total number of sperm count, and motility related parameters (de Brito et al., 2020; Ogunsuyi et al., 2020; Olugbodi et al., 2020; Santonastaso et al., 2019). These harmful effects in mammalian sperm functionality were related to NP' ability to cross blood-testis-barrier (De Jong et al., 2008; Falchi et al., 2016; Lan and Yang, 2012). However, several studies reported low physiological permeability of mammalian sperm plasma membrane to exogenous substances, as well as no intracellular uptake of NP by endocytosis due to the rigidity of sperm membrane (Barkalina et al., 2014; Falchi et al., 2016; Taylor et al., 2014, 2015). Still, toxicity occurs through direct contact of NP by binding to the sperm plasma membrane surface without intracellular uptake (Barkalina et al., 2014; Taylor et al., 2014, 2015). NP may act as surface acting agents inducing indirect toxic effects mainly due to adsorption instead of internal uptake

* Corresponding author.
E-mail address: isabeloliveira@ciimar.up.pt (I.B. Oliveira).

https://doi.org/10.1016/j.marpolbul.2022.113487
Received 7 January 2022; Received in revised form 17 February 2022; Accepted 20 February 2022
Available online 1 March 2022

(Handy et al., 2011).

Despite no information on the uptake process is found for fish sperm, their plasma membrane differs from others by presenting a high content in cholesterol and polyunsaturated lipid species, which controls the quality of sperm and varies among species (Beirão et al., 2012a; Engel et al., 2020; Labbé and Loir, 1991). This lipidic composition of the membrane increases permeability, promotes enzyme activity and intercellular membrane fusion, characteristics that allow sperm cells to fulfill their function at fertilization (Beirão et al., 2012a; Wassall and Stillwell, 2009).

Fish sperm are in a quiescent metabolic condition in the testes, characterized by an immotile state. After spawning, in fish with external fertilization, sperm faces abrupt alterations in the environmental medium (*e.g.*, alteration of osmolality and exposure to increasing oxygen), which trigger sperm activation. The osmotic pressure, namely, hyperosmotic shock, is the main factor controlling the activation of sperm motility in marine teleosts (Zilli et al., 2008). During activation, spermatozoa undergo functional modifications such as increasing membrane fluidity and motility (Alavi et al., 2019; Islam and Akhter, 2012), making them highly vulnerable. The presence of contaminants in water, such as NP, may potentiate the natural vulnerability of these cells, impairing their fertilization ability and, consequently, reproductive success.

Due to the relevance of this issue and the role of sperm in reproduction, along with the ethical advantage resulting from minimally invasive sperm collection techniques in fish, sperm quality analysis has been proposed as an indicator for reproductive success with application in environmental risk assessment (Cabrita et al., 2014; Gallo and Tosti, 2020). The most commonly used parameters to assess sperm quality are sperm count, motility pattern, viability, morphology, mitochondrial function (Erraud et al., 2017) and DNA integrity analysis (*e.g.*, through the comet assay) (Shamsi et al., 2011). Additionally, the antioxidant profile is also being used as a specific and suitable biomarker, as it can provide information on sperm vulnerability to reactive oxygen species (ROS) (Hook et al., 2014).

Accordingly, the main objective of this study was to evaluate the effects of environmentally relevant concentrations of TiO_2 NP and Ag NP on the sperm of gilthead seabream (*Sparus aurata*) upon a short-term direct exposure (*ex vivo*).

Gilthead seabream is a predator and euryhaline teleost. It is one of the most important fish species in the Mediterranean aquaculture (Nielsen et al., 2021) and a model organism in research, specifically in environmental risk assessment and cryopreservation protocols (Beirão et al., 2012a, 2012b; Marques et al., 2019). It is a protrandric sequential hermaphrodite species in which the reproductive season takes several months. One of the main advantages of using seabream is the direct and easy sampling of sperm, simply by placing a syringe outside the urogenital pore (Beirão et al., 2012b). Their spermatozoa display typical aquasperm morphology: long tail, spherical head without an acrosome, and a short or absent midpiece, as described in other fishes of the Sparidae family (Beirão et al., 2012b; Marco-Jiménez et al., 2008).

To achieve a thorough assessment of sperm quality after exposure to NP, this study adopted a multiparameter approach by evaluating sperm motility, morphometry, mitochondrial function, antioxidant responses and DNA integrity.

Understanding the spermiotoxic effects of NP' contributes to recognizing their ecological impacts. Predicting these impacts can contribute to the establishment of effective prevention measures, avoiding later recovery costs at population and community levels.

2. Materials and methods

2.1. Preparation and characterization of nanoparticle suspensions and silver nitrate solution

2.1.1. Titanium dioxide nanoparticles

TiO_2 NP, namely Aeroxide®P25 (purity ≥99.5% CAS# 13463–67-7), were provided by Sigma-Aldrich. Crystalline phase and crystallite size were identified by the X-ray diffraction technique XRD, using a Philips X'Pert X-ray diffractometer equipped with a Cu Kα monochromatic radiation source (λαK = 1.4060 nm). A stock suspension (1 mg·mL^{-1}) was prepared in distilled water (dH_2O) by sonication with an ultrasonic processor (Sonics Vibra-Cell), for 15 min (min) at 100 W, with 5:1 pulses on/off. The dispersion was performed in an ice bath. TiO_2 NP working suspensions (10, 100, 1000 and 10,000 μg·L^{-1}) were prepared with non-activated medium, namely saline solution (NaCl; 9 g·L^{-1}). The TiO_2 NP structure was confirmed by scanning transmission electron microscopy (STEM), using a JEOL 2200FS, JEOL Ltd., Japan model. TiO_2 NP size distribution in 0.9% NaCl was determined by Dynamic Light Scattering (DLS) analysis, using a ZetasizerNano ZSP (Malvern Instruments Ltd.) at 25 °C. Measurements were done in triplicate with over 13 sub-runs in fresh suspensions and also 1 h after preparation to mimic the *ex vivo* (direct exposure) conditions.

2.1.2. Silver nanoparticles and silver nitrate

Ag NP dispersion [10 nm particle size (TEM - Transmission Electron Microscopy), 0.02 mg·mL^{-1} in aqueous buffer, containing sodium citrate as stabilizer] was supplied by Sigma-Aldrich. Ag NP structure was confirmed by STEM, using a JEOL 2200FS, JEOL Ltd., Japan model. DLS analysis was performed to determine Ag NP behavior in 0.9% NaCl, as previously described for TiO_2 NP.

Ag NP stock suspension (0.0025 mg·mL^{-1}) was prepared in dH2O and Ag NP working suspensions (0.25, 25 and 250 μg·L^{-1}) were prepared in 0.9% NaCl. Stock and working suspensions were vortexed before the next dilution.

To allow the discrimination of the involvement of dissolved Ag form on the measured responses, Ag^+ solutions were also prepared (see Section 2.3.). $AgNO_3$ (purity ≥99%, ACS reagent, CAS# 7761-88-8) was provided by Sigma-Aldrich. $AgNO_3$ stock solution (0.0040 mg·mL^{-1}, [Ag^+] = 0.0025 mg·mL^{-1}) was prepared in dH_2O and $AgNO_3$ working solutions (0.40, 40, 400 μg·L^{-1}, [Ag^+] = 0.25, 25 and 250 μg·L^{-1}) were prepared in 0.9% NaCl by successive dilutions of the stock suspension, as previously performed for Ag NP. Stock and working suspensions were vortexed before proceeding with the next dilution. We will refer to the use of Ag^+ present in $AgNO_3$ as Ag^+.

2.2. Semen collection

Sperm was collected from sexually mature gilthead seabream (*Sparus aurata*) reared males (2 years old, approximately 0.5 kg), provided by Aqualvor Lda fish farm (Lagos, Portugal) during their reproductive season (December–February in the South of Portugal). Sperm was released by abdominal massage and retrieved with a 1 mL syringe, without the needle. Samples were kept in microtubes inside polystyrene support to avoid direct contact with ice (~4 °C), until analysis. All samples showing urine contamination were rejected. A total of 12 sperm samples corresponding to different males were used.

2.3. Experimental design

Semen was directly exposed (*ex vivo*) to several concentrations of TiO_2 NP or Ag NP, in two independent trials. TiO_2 NP tested concentrations reflected the levels found at Mediterranean marine waters (water column and top surface layer) (Labille et al., 2020), as well as supra-environmental concentrations. Ag NP levels replicated the levels found in French wastewater (influent and effluent) (Deycard et al., 2017) and supra-environmental concentrations. Four concentrations of TiO_2 NP (10, 100, 1000 and 10,000 μg·L^{-1}) and three concentrations of Ag NP (0.25, 25 and 250 μg·L^{-1}) were tested. Since Ag NP can undergo oxidative dissolution in water (Zhang et al., 2016), the same concentrations of Ag^+ (0.25, 25 and 250 μg·L^{-1}) were also assessed to evaluate the contribution of the dissolved Ag form. The *ex vivo* exposures (1:10, v/v semen and exposure medium [0.9% NaCl and NP], respectively to

achieve a final sperm concentration of ~2 × 10^7 cells/mL) lasted 1 h with gentle agitation performed every 15 min. The exposure was performed at 4 °C to avoid sperm degradation (Gallego and Asturiano, 2019).

After exposure, sperm was directly collected for motility (Section 2.4) and morphometry (Section 2.5) evaluation. For the remaining analysis, samples were centrifuged in a refrigerated centrifuge (Eppendorf 5415R) at 800*g* for 15 min at 4 °C, and the supernatant was discarded to remove NP and seminal plasma. Then, the pellet was resuspended in 0.9% NaCl to achieve a final concentration of 2 × 10^7 cells·mL^{-1} and divided into several aliquots for further evaluation.

2.4. Sperm motility

Motility was assessed using the CASA system (ISAS - Integrated System for Sperm Analysis; Proiser, Valencia, Spain) coupled to a phase-contrast microscope (Nikon E-200; Nikon, Tokyo, Japan) with an ISAS camera (Gallego and Asturiano, 2018, 2019). For sperm activation, 5 μL of artificial seawater (1100 mOsm·kg^{-1}) were added to 1 μL of the cell suspension and motility was recorded at 15, 30, 45, and 60 s post-activation in the same field. Samples exposed to each NP and concentration (n = 12 males) were analyzed four times per treatment. Image sequences were captured with a 10× negative phase contrast objective, saved and analyzed afterwards using the ISAS software. The software settings were adjusted to gilthead seabream sperm using 25 frames per second and considering the head area of 1 to 90 μm^2. Spermatozoon was considered motile when VCL (curvilinear velocity) was higher than 10 μm·s^{-1}. CASA rendered the percentage of motile cells in the sperm sample. The assessed parameters were: the total motility (TM, %), expressed as the percentage of motile cells, and the curvilinear velocity (VCL, mm/s), which corresponds to the average velocity of a spermatozoon head along its curvilinear trajectory (Gallego et al., 2014).

2.5. Sperm morphometry

Seabream sperm were analyzed for morphometric changes using the protocol developed by Marco-Jiménez et al. (2008). Briefly, after exposure to NP, 4 μL of sperm were fixed in a 1:50 ratio (v:v) in 2.5% glutaraldehyde solution prepared in PBS. An aliquot of the previous dilution was then placed in a slide and visualized using a 100 x·negative phase contrast objective, using immersion oil (Nikon Plan Fluor) in an Eclipse E400 Nikon microscope connected to an ISAS camera. Images were acquired and the morphometric parameters were analyzed using the computer-assisted sperm analysis (ASMA - Automated Sperm Morphometry Analysis) software (Sperm Class Analyser, Morfo Version 1.1, Valencia, Spain). The morphometric parameters determined in the sperm head were: head length (μm), width (μm), perimeter (μm), and area (μm^2). A total of 200 sperm cells were analyzed per male (n = 10) and treatment.

2.6. Sperm DNA integrity

An aliquot of each sample was diluted in 0.9% NaCl to a final concentration of 1 × 10^4 cells·mL^{-1}. Comet assay was performed according to Collins (2004), adapted with a system of eight gels per slide as described by Guilherme et al. (2014) and adapted for gilthead seabream sperm according to Cabrita et al. (2005). Briefly, the slides were immersed in a lysis solution (2.5 M NaCl, 100 mM EDTA, 10 mM Tris, 1% Triton X-100, and 1% lauryl sarcosine, pH 10) at 4 °C for 1 h. Dithiothreitol (10 mM) was added to the lysis solution and gels were immersed for 30 min at 4 °C. Subsequently, lithium diiodosalicylate (4 mM), was added to the solution and gels were immersed for 90 min at 4 °C.

Slides were then placed horizontally in the electrophoresis tank with electrophoresis solution (0.3 M NaOH, 1 mM Na2–EDTA, pH 12) for 20 min at 4 °C. Electrophoresis was conducted at a fixed voltage of 20 V, a current of 300 mA for 10 min at 4 °C.

Afterwards, slides were drained and immersed in a neutralizing solution (0.4 M Tris, pH 7.5) for 5 min at 4 °C. This procedure was performed twice and slides were then placed in a solution of 70% ethanol for 2 min, 90% ethanol for 2 min and followed by pure ethanol for 2 min. Lastly, slides were left to dry in the air and stored for later analysis. Positive control was also prepared in 0.9% NaCl and previously incubated with a damage promoter [hydrogen peroxide (H_2O_2) 50 mM] for 15 min at 4 °C (Azqueta et al., 2011).

For comet visualization, slides were stained with ethidium bromide (20 μg·mL^{-1}). Fifty nucleoids were observed per gel, using a Leica DM2000 LED fluorescence microscope (x400 magnification). DNA damage was quantified by visual scoring of nucleoids, according to Collins (2004). Nucleoids were scored into five classes according to the tail length and intensity, from 0 (no tail) to 4 (almost all DNA in tail indicating highly damaged DNA). The genetic damage indicator (GDI) was calculated according to the formula:

$$\mathrm{GDI} = \sum \%\text{nucleoids class } i \times i$$

where i is the number of each defined class (ranging within 0–4) and GDI values were inherently expressed as arbitrary units on a scale of 0–400 per 100 scored nucleoids.

2.7. Sperm mitochondrial function and antioxidant activity

Mitochondrial function was evaluated as described by Oliveira et al. (2008) with some modifications for gilthead seabream. Briefly, we evaluated mitochondrial function by using Rhodamine 123/propidium iodide (Rh123/PI) dual fluorescent staining. Rh123 is a cationic fluorescent dye (1 mg·mL^{-1} in methanol [−20 °C]) was diluted in dH_2O to a concentration of 0.1 mg·mL^{-1} and 10 μL were added to 400 μL of each cell suspension (1 to 2 × 10^7 cells·mL^{-1}). Samples were incubated at 4 °C for 30 min, in the dark, allowing Rh123 to accumulate in functional active mitochondria. Afterwards, samples were centrifuged for 10 min at 500*g*, the supernatant was discarded and the pellet was resuspended in NaCl. Then, 10 μL of PI (0.1 mg·mL^{-1}), used to mark unviable cells, were added to the sample 5 min before flow cytometric analyses (Attune® Acoustic Focusing Cytometer, ThermoFisher Scientific). The instrument was equipped with a blue laser (488 nm) for excitation. Green fluorescence from Rh123 was detected in BL1 sensor, through a 530/30 filter, while the red fluorescence of PI was collected through a 574/26 filter. Sperm cells were gated based on the forward (FS) *vs.* side scatter (SC) properties. At least 10, 000 events were acquired for each sample. The percentage of sperm with functional mitochondria was calculated as the ratio of cells positive for Rh123 (PI+Rh123+/PI-Rh123+) *vs.* total cell number.

For the biochemical analysis, spermatozoa were lysed to release antioxidants. First, sperm samples were centrifuged at 4 °C for 10 min at 10000*g*, and the supernant was discarded. Then, the pellet was resuspended with PBS 0.1% Triton X-100, vortexed and frozen in liquid nitrogen. Afterwards, samples were thawed at room temperature, centrifuged at 5000*g* for 5 min at 4 °C, and the supernatant removed. Lastly, samples were diluted with 0.01 M PBS and subsequently frozen in liquid nitrogen and stored at −80 °C until analyses.

Catalase (CAT) activity analysis was based on those described by Claiborne (1985) and Giri et al. (1996). Briefly, the assay mixture consisted of 10 μL phosphate buffer (0.05 M, pH 7.0), 195 μL hydrogen peroxide (10 mM) and 10 μL of the sample. The absorbance was monitored for 3 min at intervals of 10 s at 25 °C. The CAT activity was analyzed at 240 nm and expressed in μmol H_2O_2 consumed·min^{-1}.mg $protein^{-1}$ (ε = 43.5 M^{-1} cm^{-1}).

Glutathione peroxidase (GPx) activity was assayed according to the method described by Mohandas et al. (1984), modified by Athar and Iqbal (1998). The assay mixture consisted of 90 μL phosphate buffer (0.05 M, pH 7.0), X mL EDTA (10 mM), 30 μL sodium azide (10 mM), 30

μL glutathione reductase (GR; 2.4 U/mL), 30 μL reduced glutathione (GSH; 10 mM), 30 μL NADPH (1.5 mM), 30 μL H_2O_2 (2.5 mM) and 30 μL of the sample. The absorbance was read at 340 nm each 30 s for a 5 min period at 25 °C and expressed in nmol NADPH oxidized·min^{-1}.mg protein^{-1} ($\varepsilon = 6.22 \times 10^3$ M^{-1} cm^{-1}).

Superoxide dismutase (SOD) activity was determined through the spectrophotometric enzymatic kit (RANSOD TM, Randox), adapted to a microplate. Xanthine and xanthine oxidase were used to produce superoxide radicals that react with 2-(4-iodophenyl)-3-(4-nitrophenol)-5-phenyltetrazolium chloride (INT) originating a red dye of formazan. The assay consisted in adding 10 μL of diluted PMS, 210 μL of Mixed substrate (R1) and 30 μL of xanthine oxidase (R2) .The absorbance was read at 550 nm during 3:30 min at 25 °C. SOD activity was expressed in U·mg protein^{-1}, where a unit of SOD induced the inhibition of 50% of the INT reduction rate.

The total protein content was determined in the PMS according to Bradford (1976), adapted to a microplate, using bovine serum albumin as a standard. Absorbance reading was performed at 595 nm.

All antioxidants and proteins were measured using a microplate reader (Synergy™ H1 BioTeck®).

2.8. Statistical analyses

The effect of the different treatments (independent variables) on the different dependent variables (motility, morphometry, GDI, DNA damage classes, enzymatic antioxidants, and mitochondrial function) was analyzed using one-way ANOVA, followed by a multiple comparisons test. Graphical validation tools were used to verify ANOVA assumptions. Whenever assumptions were not fulfilled, data were evaluated with the equivalent non-parametric test. To satisfy the assumptions of ANOVA, percentage data (*viz.*, sperm motility and mitochondrial function) were arcsine-transformed. A paired-samples *t*-test, and the equivalent non-parametric (Mann-Whitney *U* test), was conducted to distinguish the effects of Ag NP from those of Ag^+.

The results were expressed as mean and standard deviation. The statistical analyses were performed using IBM.SPSS®, version 27.0.1, and all the statistical tests were considered significant when $p < 0.05$. All the descriptive data have been collated into supplementary tables.

3. Results

3.1. Characterization of the nanoparticle suspensions

3.1.1. Titanium dioxide nanoparticles

The standard spheroid irregular shape of TiO_2 NP (Aeroxide© P25) with a primary size of a mean particle diameter of 19.34 ± 6.72 nm in the stock suspension was confirmed by STEM (Fig. S1). The histograms of the different sizes of TiO_2 NP showed a unimodal right-skewed distribution, with approximately 60% of the values ranging from 10 to 20 nm in the stock suspension, as well as in all TiO_2 NP working suspensions. The XRD analysis demonstrated the presence of the crystalline phase anatase (86.8%) and rutile (13.2%). DLS analysis of TiO_2 NP stock suspension (1 mg·mL^{-1}) in dH_2O showed the presence of agglomerates with an average size of NP of 189.0 ± 80.2 nm. The mean hydrodynamic diameters of TiO_2 NP agglomerates in the tested suspensions (in NaCl) were 235.32 ± 17.35, 239.84 ± 63.98, 252.46 ± 51.76 and 690.95 ± 121.59 nm at 10, 100, 1000 and 10,000 μg·L^{-1}, respectively.

3.1.2. Silver nanoparticles

STEM analysis showed that silver dispersion (stock suspension) had a spherical appearance with a mean primary size particle diameter of 21.50 ± 8.27 nm (Fig. S2). The histogram of the frequency distribution of different sizes of Ag NP showed a unimodal right-skewed distribution, with nearly 35, 55, and 80% of the values ranging from 10 to 20 nm in the stock suspension and Ag NP working suspensions of 250 μg·L^{-1} and 25 μg·L^{-1}, respectively. For the 0.25 μg·L^{-1} working suspension of Ag NP, 87.50% of the values ranged from 4 to 10 nm. DLS analysis of Ag NP stock suspension (0.0025 mg·mL^{-1}) in dH_2O revealed the presence of agglomerates with an average size of 142.73 ± 13.74 nm. The mean size of the agglomerates in the tested suspensions (in NaCl) was 130.52 ± 7.89, 134.29 ± 42.28 and 230.04 ± 32.57 nm for 0.25, 25, and 250 μg·L^{-1}, respectively.

3.2. Sperm motility and morphometry

The CASA system analysis, carried out at different time points (15, 30, 45, and 60 s post-activation), showed that increasing concentrations of TiO_2 NP did not affect sperm TM, as no significant differences were observed among groups (Table S1; Fig. 1A). Similar to TM, VCL also did not show significant differences (Table S1; Fig. 2A).

Concerning Ag NP exposure, TM decreased in the highest concentration in comparison with the control group, for all the different time points post-activation (Table S2). TM remained unaltered after the exposure of sperm to Ag^+ in all the recorded post-activation times (Table S2; Fig. 1B). TM was similar between the corresponding exposure levels Ag NP and Ag^+ (Table S3). VCL decreased in the highest Ag NP concentration concerning to the intermediate concentration, at 15 s post-activation ($H_{(3,40)} = 8.629$, $p \leq 0.05$), while in the other post-activation times, VCL remained unaltered. After the exposure to Ag^+, VCL also remained unaltered in all recorded post-activation times (Table S2). For the concentration 25 μg·L^{-1} at 30 s post-activation ($U_{(1,16)} = 11.000$, $p \leq 0.05$) and 250 μg·L^{-1} at 45 s post-activation ($U_{1,16)} = 11.500$, $p \leq 0.05$) the VCL was lower for Ag^+ than for Ag NP (Fig. 2B).

The morphometric analysis showed no significant differences for any of the studied parameters after exposure to all NP tested, TiO_2 and both Ag NP and Ag^+ (Tables S1 and S2; Fig. 3). The absence of differences between Ag NP and Ag^+ was also observed for all the morphometric parameters (Table S3).

3.3. DNA integrity in sperm

After TiO_2 NP exposure, gilthead seabream sperm did not show significant alterations in the GDI among treatments (Table S1; Fig. 4A). To better understand the distribution of DNA damage throughout the range of the tested concentrations, GDI classes were analyzed individually. Again, no statistically significant differences were observed between treatments in all classes (Table S1). Similarly to TiO_2 NP, no significant alterations in the GDI values among treatments were found for Ag NP or Ag^+ (Table S2; Fig. 4B) as well as for DNA damage classes (Table S2). No significant differences were found between each concentration of Ag NP and Ag^+ for GDI (Table S3), nor for all assessed DNA damage classes (Table S3).

3.4. Sperm mitochondrial function and antioxidant activity

No significant differences were detected between the mitochondrial function of sperm exposed to TiO_2 NP and the control treatment, as well as among the tested TiO_2 NP concentrations (Table S1; Fig. 5A). The same result was observed for Ag NP and Ag^+ (Table S2; Fig. 5B). The paired samples, between each concentration of Ag NP and Ag^+, presented no significant differences (Table S3).

The studied antioxidants (CAT, GPx and SOD) showed decreased activities in all TiO_2 NP treatments in comparison with control ($H_{(4,46)} = 17.381$, $p = 0.002$; $H_{(4,45)} = 17.721$, $p \leq 0.001$; $H_{(4,46)} = 18.654$, $p \leq 0.001$ for CAT, GPx, and SOD respectively) (Table S1; Fig. 6A, C, E). CAT and GPx activities remained unaltered after the exposure of sperm to Ag NP (Fig. 6B, D), though the activity of SOD decreased significantly in the two lowest Ag NP concentrations relatively to control ($H_{(3,36)} = 8.401$; $p \leq 0.05$) (Table S2; Fig. 6F).

When sperm cells were exposed to Ag^+, CAT activity decreased significantly in both the lowest and the highest concentrations relatively

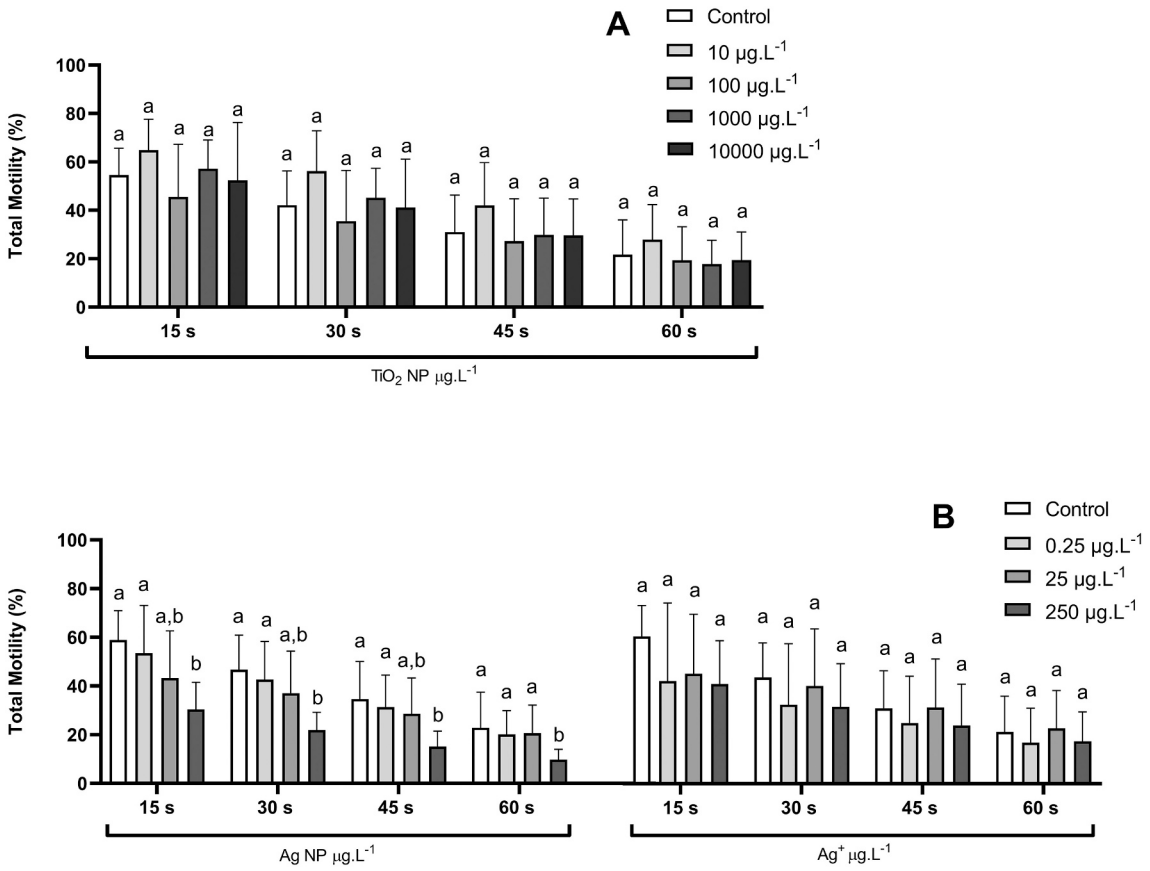

Fig. 1. Total motility (%) in spermatozoa of *S. aurata* exposed for 1 h to (A) titanium dioxide nanoparticles (TiO_2 NP: 10, 100, 1000 and 10,000 µg·L^{-1}), as well as (B) silver nanoparticles (Ag NP: 0.25, 25 and 250 µg·L^{-1}) and silver as $AgNO_3$ ([Ag^+]: 0.25, 25 and 250 µg·L^{-1}). Total motility was recorded 15, 30, 45, and 60 s post-activation. Different lower-case letters denote significant differences ($p < 0.05$). Columns correspond to mean values and error bars represent the standard deviation.

to control ($H_{(3,40)} = 16.518$; $p \leq 0.001$) (Table S2; Fig. 6B), while a significant decrease was observed in the GPx activity of sperm exposed to the lowest concentration of Ag^+ ($H_{(3,36)} = 14.700$; $p \leq 0.01$) (Table S2; Fig. 6D). SOD activity decreased significantly in the lowest and intermediate Ag^+ concentrations in relation to control ($H_{(3,40)} = 17.530$; $p \leq 0.001$) (Table S2; Fig. 6F).

The paired-sample *t*-test showed that CAT activity was lower in the highest Ag^+ concentration ($U_{(1,20)} = 20.000$; $p \leq 0.05$) (Table S3; Fig. 6B). In the case of SOD, lower activity was also found for both the lowest and the highest concentrations of Ag^+ ($U_{(1,18)} = 15.000$; $p \leq 0.05$; $U_{(1,20)} = 20.000$; $p \leq 0.05$for 0.25 and 250 µg·L^{-1}, respectively) (Table S3; Fig. 6F). No differences were found between Ag NP and Ag^+ for GPx activity (Table S3; Fig. 6D).

4. Discussion

The importance of addressing sperm quality for environmental risk assessment was just recently acknowledged. Sperm quality is intrinsically related to the fertilization ability being crucial for species maintenance and propagation. Thus, understanding contaminant effects and mode of action in sperm allows reliably predicting the environmental risk posed by these substances and setting recommendations regarding their presence in the environment. Notwithstanding the suitability of sperm quality, namely motility, as an indicator of reproductive success with application in environmental risk assessment, a limited number of studies exist focusing on the impact of contaminants on sperm function (Gallego and Asturiano, 2018, 2019; Gallo et al., 2020), particularly those related to the effects of NP in aquatic organisms. Despite that, the existing information points towards the impairment of sperm function after exposure to NP (Gallo et al., 2016; Han et al., 2019; Kowalska-Góralska et al., 2019; Özgür et al., 2018a, 2018b, 2018c, 2019, 2020).

4.1. Sperm motility and morphometry

The majority of the physiological processes of fish sperm is determined by motility as fertilization relies on sperm encounters with the oocyte (Cosson, 2019). For that reason, this is the most studied functional parameter in sperm.

The effects of iron oxide NP (Fe_3O_4 NP), zinc oxide NP (ZnO NP), silica oxide NP (SiO NP), and copper oxide NP (CuO NP) in freshwater and marine fish sperm showed a general reduction of motility after *ex vivo* short-term exposures (Kowalska-Góralska et al., 2019; Özgür et al., 2018b, 2018c, 2019). The same occurred after TiO_2 NP *ex vivo* exposures in marine organisms (fish - *Capoeta trutta* and bivalve -*Tegillarca granosa*). These studies showed a general decrease in different motility parameters (VCL, straight-line velocity – VSL, and angular path velocity – VAP) after 2 h of direct exposure to TiO_2 NP (10 to 10,000 µg·L^{-1} of TiO_2 NP) (Han et al., 2019; Özgür et al., 2020). On the contrary, our results revealed no alteration of the motility parameters (TM and VCL) following TiO_2 NP exposure, despite the adoption of the same exposure procedure (direct exposure) and the same range of TiO_2 NP concentrations (10 to 10,000 µg·L^{-1} of TiO_2 NP). In the case of the rainbow trout (*Oncorhynchus mykiss*), Özgür et al. (2018a) also reported no alteration in VCL after 3 h of direct exposure to TiO_2 NP concentrations ranging from 10 to 50,000 µg·L^{-1}. However, these authors found contradictory results for the remaining parameters (VAP, VSL and percentage of linearity). The discrepancies between studies may be due to the duration of exposure, different sensitivity among the assessed parameters, and species-specificities. Distinct species-specific mechanisms were already reported, pointing towards a higher inherent vulnerability of freshwater

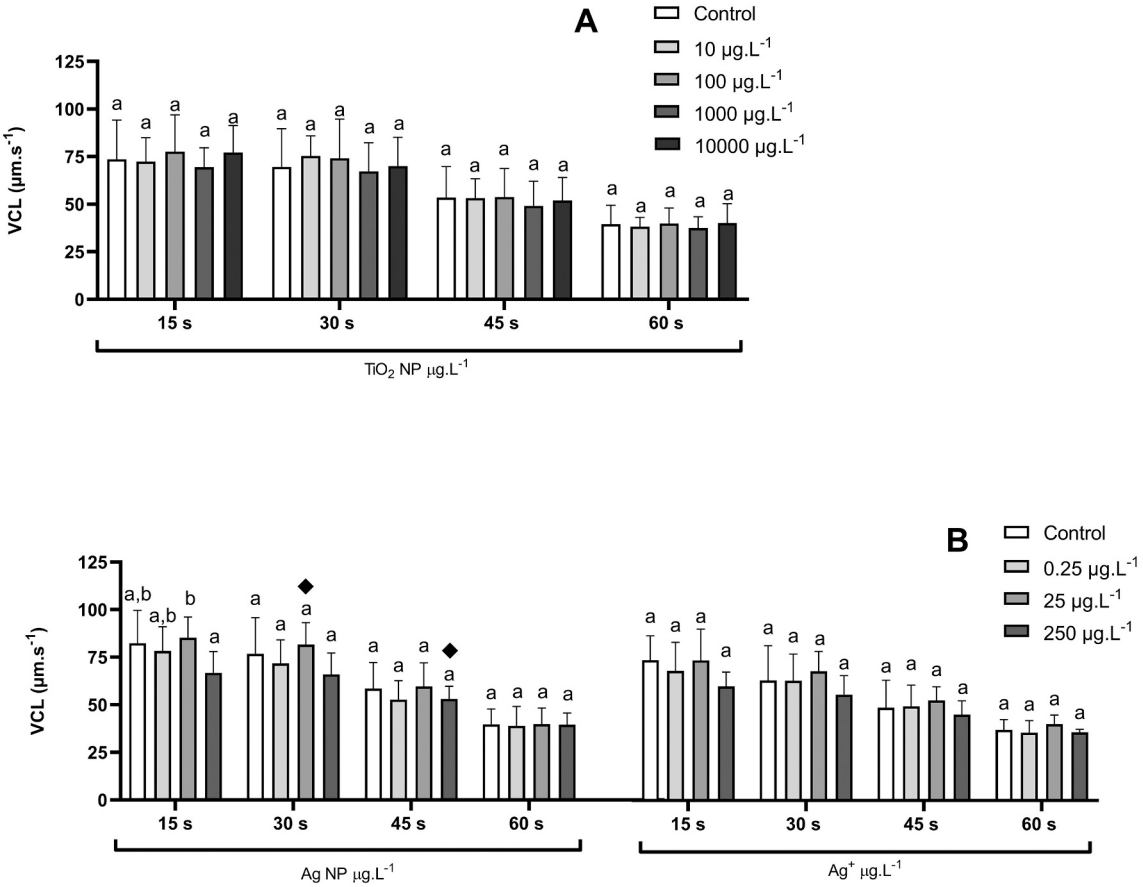

Fig. 2. Curvilinear velocity (VCL) ($\mu m \cdot s^{-1}$) in spermatozoa of *S. aurata* exposed for 1 h to (A) titanium dioxide nanoparticles (TiO_2 NP: 10, 100, 1000 and 10,000 $\mu g \cdot L^{-1}$), as well as (B) silver nanoparticles (Ag NP: 0.25, 25 and 250 $\mu g \cdot L^{-1}$) and silver as $AgNO_3$ ([Ag^+]: 0.25, 25 and 250 $\mu g \cdot L^{-1}$). VCL was recorded 15, 30, 45, and 60 s post-activation. Different lower-case letters denote significant differences among treatments ($p < 0.05$). Significant differences between the corresponding concentrations of Ag NP and Ag^+ is depicted by (◆) ($p < 0.05$). Columns correspond to mean values and error bars represent the standard deviation.

sperm due to their physiological maladaptation to hypoosmotic shock (Billard and Cosson, 1990). Moreover, marine fish have a higher poly-unsaturated/unsaturated fatty acids ratio than freshwater fish (Drokin, 1993), which confers higher fluidity to marine fish sperm membranes and thus higher resistance.

To the best of our knowledge, no studies assessed the effects of Ag NP in the motility of marine organisms' sperm. The available data focused on humans (short-term direct exposure) and other mammals (long-term *in vivo* exposure), reporting a general decrease in sperm motility (TM, VCL, VSL, and VAP) (Moretti et al., 2013; Olugbodi et al., 2020; Shehata et al., 2021; Wang et al., 2017). Similarly, in the present study, TM also decreased, but only at the highest Ag NP concentration (250 $\mu g \cdot L^{-1}$). The sperm motility of gilthead seabream might be regulated by ROS-mediated processes (Zilli et al., 2017). The decrease in motility after exposure to the highest Ag NP concentration is not accompanied by DNA damage, impairment of the mitochondrial function nor alteration in the antioxidants (see Section 4.3). Thus, we anticipate that Ag NP might affect motility by a physical interaction with the sperm surface. We hypothesize two different mechanisms: impairment of the motility by mechanical processes or by interactions of the Lewis-acid of the NP surface with Lewis-acid thiol groups of the membrane (Taylor et al., 2014). Mechanical processes induced by the large agglomerates attached to the flagellum may delay motility, whereas NP interaction with the membrane structure/composition may interfere with membrane transporters. Taylor et al. (2014) suggested that gold NP affected the motility of bull sperm by interacting with the membrane.

The higher toxicity of the Ag ion was previously described for zebrafish gills (*Danio rerio;* exposure *via* water for 48 h) (Griffitt et al., 2009) and the marine diatom (*Chaetoceros curvisetus*) (Lodeiro et al., 2017). However, the higher toxicity of the Ag ion compared to Ag NP was not possible to confirm since no alterations of the motility were found for Ag^+.

Like motility, sperm morphometry is a reliable indicator of sperm quality (Gallego et al., 2014; Marco-Jiménez et al., 2008). Any alterations in its shape may interfere with the swimming capacity or the penetration of the sperm head through the oocyte micropyle. Our results showed that the analyzed head morphometric parameters were unaltered after TiO_2 NP, Ag NP and Ag^+ exposure. No studies were found regarding using this tool to describe the effects of NP in sperm. Nevertheless, a single study with goldfish (*Carassius auratus*) showed no effects on sperm head length, width and area after an instant exposure (5 s) to mercury (1 to 100,000 $\mu g \cdot L^{-1}$). However, the levels of those parameters increased after 24 h exposure (Van Look and Kime, 2003), suggesting that morphometric changes are time-dependent and that instant exposures are not likely to induce alterations. We forecasted the absence of alterations in sperm morphometry was related to no or slight motility effects induced by TiO_2 NP and Ag NP exposure, respectively. Plus, sperm was exposed in its quiescent stage (see Section 4.4), as gilthead seabream sperm motility only lasts a few minutes.

Exposing non-motile sperm, though not fully mimicking the post-release moment, is the trade-off to going deeper into the effects of water contaminants on these cells. We, therefore, predict that these *ex vivo* assays reflect the impacts of NP at the post-release moment without underestimating the risk to spermatozoa and its ecological consequences.

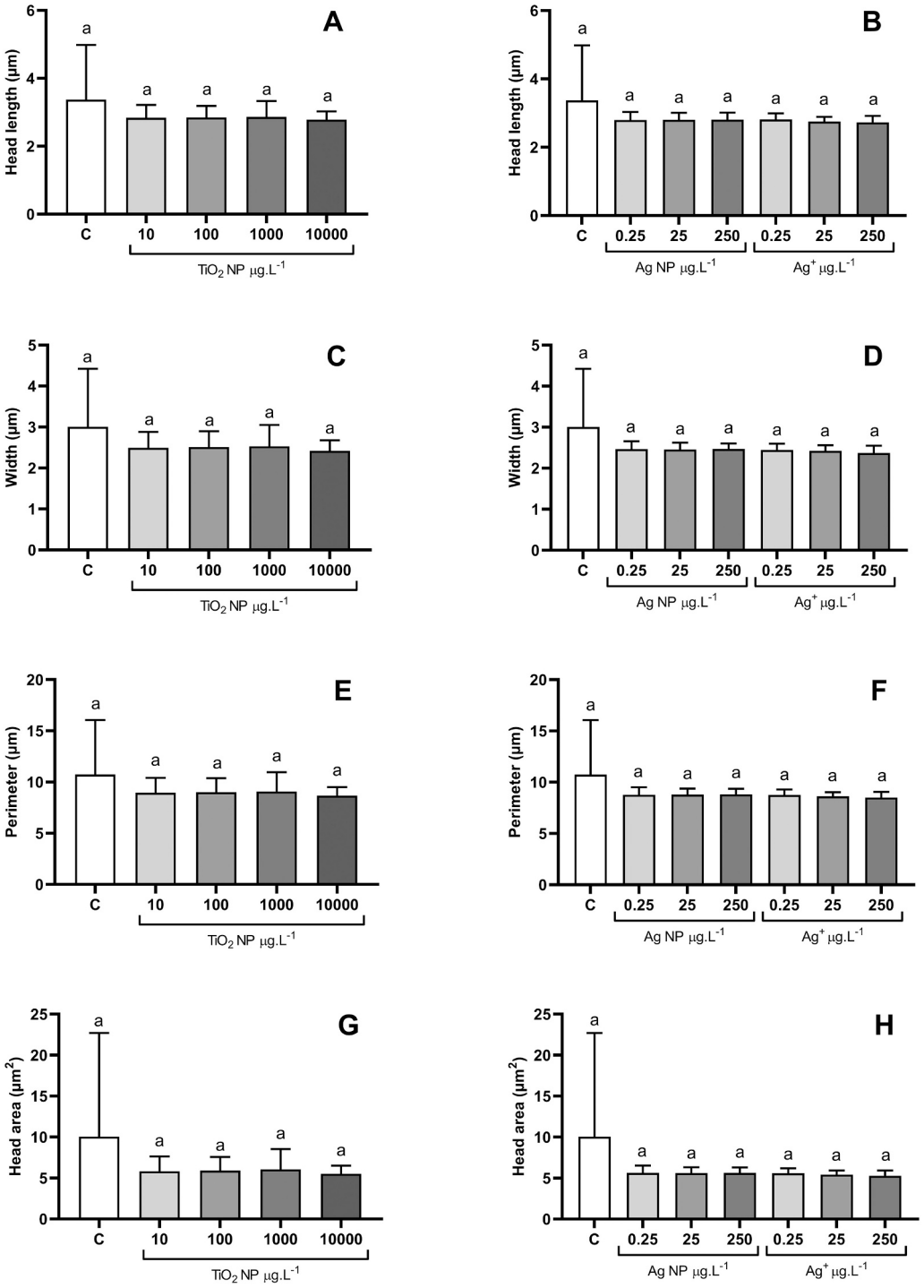

Fig. 3. Morphometric parameters (μm^2) in spermatozoa of *S. aurata* exposed for 1 h to titanium dioxide nanoparticles (TiO_2 NP: 10, 100, 1000 and 10,000 $\mu g \cdot L^{-1}$), as well as silver nanoparticles (Ag NP: 0.25, 25 and 250 $\mu g \cdot L^{-1}$) and silver as $AgNO_3$ ([Ag^+]: 0.25, 25 and 250 $\mu g \cdot L^{-1}$). Different lower-case letters denote significant differences ($p < 0.05$). Columns correspond to mean values and error bars represent the standard deviation. C - control.

4.2. Sperm DNA integrity

Assessing DNA damage at individual levels allows predicting any changes at the population level. The loss of DNA integrity was previously reported in the sperm of humans and aquatic organisms following direct exposure to NP (Gallo et al., 2016, 2018; Han et al., 2019; Santonastaso et al., 2019, 2020; Wang et al., 2017). DNA damage was reported even at low TiO_2 NP concentrations in human sperm (1, 10 $\mu g \cdot L^{-1}$) and in a marine bivalve (10 and 100 $\mu g \cdot L^{-1}$) (Santonastaso et al., 2019; Han et al., 2019). Unlike these studies, no DNA damage occurred for the seabream sperm suggesting less vulnerability to this NP. The lower vulnerability of seabream sperm compared with the marine bivalve may be because the sperm of bivalves are active when exposed to NP, as they are motile for more than 24 h. Sessile organisms exhibit extensive periods of sperm motility than fish, as their spermatozoa must travel longer distances to find the egg to fertilize (Gallego et al., 2014). The same can be considered for human sperm since assays use ejaculated sperm and, therefore, motile cells.

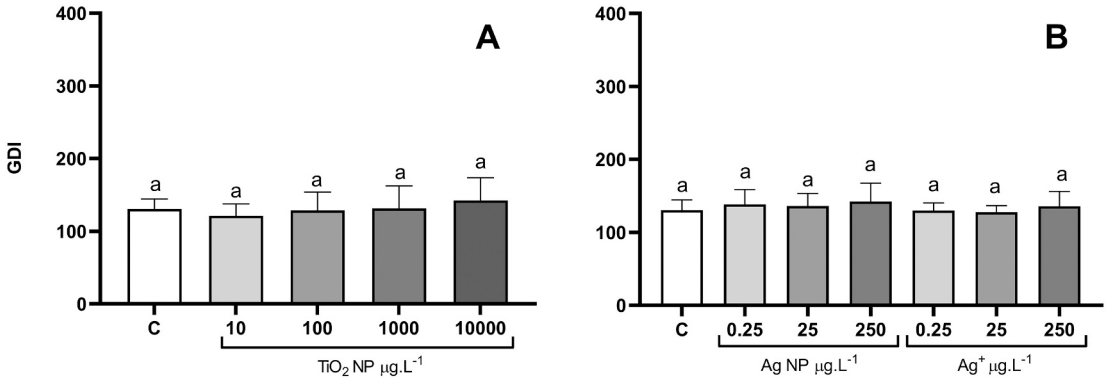

Fig. 4. Genetic damage indicator (GDI; expressed in arbitrary units) in spermatozoa of *S. aurata* exposed for 1 h to (A) titanium dioxide nanoparticles (TiO_2 NP: 10, 100, 1000 and 10,000 µg·L^{-1}), as well as (B) silver nanoparticles (Ag NP: 0.25, 25 and 250 µg·L^{-1}) and silver as $AgNO_3$ ([Ag^+]: 0.25, 25 and 250 µg·L^{-1}). Different lower-case letters denote significant differences ($p < 0.05$) in relation to control. Columns correspond to mean values and error bars represent the standard deviation. C - control.

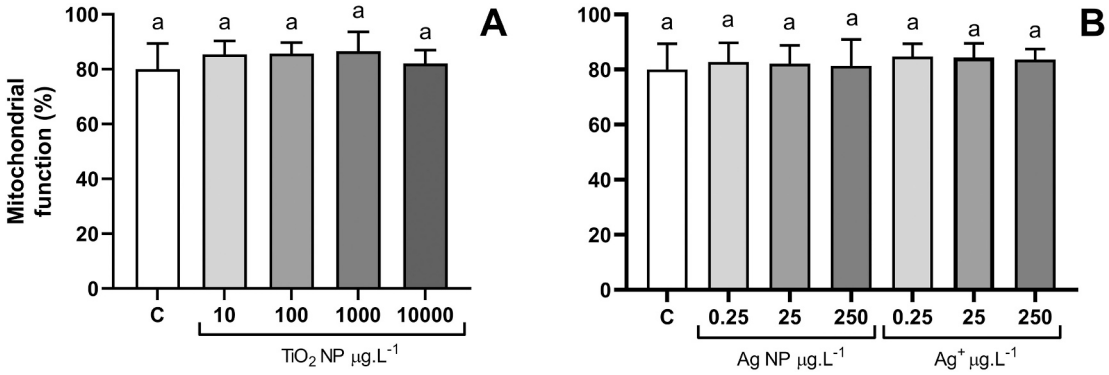

Fig. 5. Mitochondrial function (PI+Rh123+/PI-Rh123+) in spermatozoa of *S. aurata* exposed for 1 h to (A) titanium dioxide nanoparticles (TiO_2 NP: 10, 100, 1000 and 10,000 µg·L^{-1}), as well as (B) silver nanoparticles (Ag NP: 0.25, 25 and 250 µg·L^{-1}) and silver as $AgNO_3$ ([Ag^+]: 0.25, 25 and 250 µg·L^{-1}). Different lower-case letters denote significant differences ($p < 0.05$). Columns correspond to mean values and error bars represent the standard deviation. C - control.

In the case of Ag NP, there are no comparable studies on aquatic organisms. However, a decrease in DNA integrity occurred after direct exposure (1 h) of human sperm to high concentrations of Ag NP (200,000 µg·L^{-1} and 400,000 µg·L^{-1}) (Wang et al., 2017). Contrary to human sperm, no DNA damage occurred in our study with sperm of gilthead seabream after exposure to Ag NP (0.25 to 250 µg·L^{-1}) and Ag^+ ion (0.25 to 250 µg·L^{-1}). Yet, the disparity of concentrations between studies does not allow further comparisons.

4.3. Sperm mitochondrial function and antioxidant activity

ROS formation is the predominant molecular mechanism of NP toxicity to sperm, which induces impairment of the mitochondrial function and changes in membrane composition (Gallo et al., 2016, 2018; Özgür et al., 2018b, 2020; Ogunsuyi et al., 2020). The vulnerability towards ROS is related to the sperm plasma membrane high content of cholesterol and polyunsaturated fatty acids (Costantini et al., 2010). Plus, the small volume of cytoplasm and thus the low levels of antioxidants depicted by sperm contribute to their susceptibility to ROS and oxidative stress (Słowińska et al., 2013).

In this work, SOD activity decreased after exposure to low and intermediate concentrations of Ag NP, and an overall depletion of the antioxidant activity (CAT, GPx, and SOD) occurred after exposure to TiO_2 NP. As antioxidants are the first line of defense against ROS (Costantini et al., 2010; Słowińska et al., 2013), their depletion might suggest that gilthead seabream spermatozoa are vulnerable to ROS production.

The excess of ROS might inhibit the enzymes of oxidative phosphorylation and glycolysis, limiting the production of ATP (De Lamirande et al., 1997) and subsequently impairing mitochondrial function. Therefore, concomitantly to the depletion of the activity of antioxidants, it was expected to find impairment of the mitochondrial function of sperm exposed to the NP. Yet, no alteration of the mitochondrial function emerged after exposure to NP. The absence of mitochondrial impairment may be due to the quiescent stage of spermatozoa during the *ex vivo* exposures. In quiescent spermatozoa, mitochondria are at a basal metabolic rate encompassing low energy mobilization, low oxygen consumption (Alavi et al., 2019), and inhibition of some enzymes that regulate the respiratory chain (Christen et al., 1987). Plus, in quiescent spermatozoa, no interference of the ROS-mediated signal cascade, that triggers activation, occurred. Hence, the depletion of the antioxidants suggests two possible mechanisms of action by the NP: enzyme inhibition by NP, more severe in the case of TiO_2 NP, or by the promotion of a favourable antioxidant condition. Indeed, both TiO_2 NP and Ag NP can have antioxidant properties, a characteristic that depends on the extracts used in their synthesis (Keshari et al., 2020; Bedlovičová et al., 2020; Rajeswari et al., 2021). For Ag NP these mechanisms are concentration-dependent, as it does not occur at the highest concentration.

Previous studies reported increasing lipid peroxidation either in fish spermatozoa directly exposed to TiO_2 NP or in the testis of rats after long-term oral exposure to Ag NP (Özgür et al., 2020; Shehata et al., 2021). Assessment of lipid damage would have been convenient in our samples but was not possible due to methodological limitations.

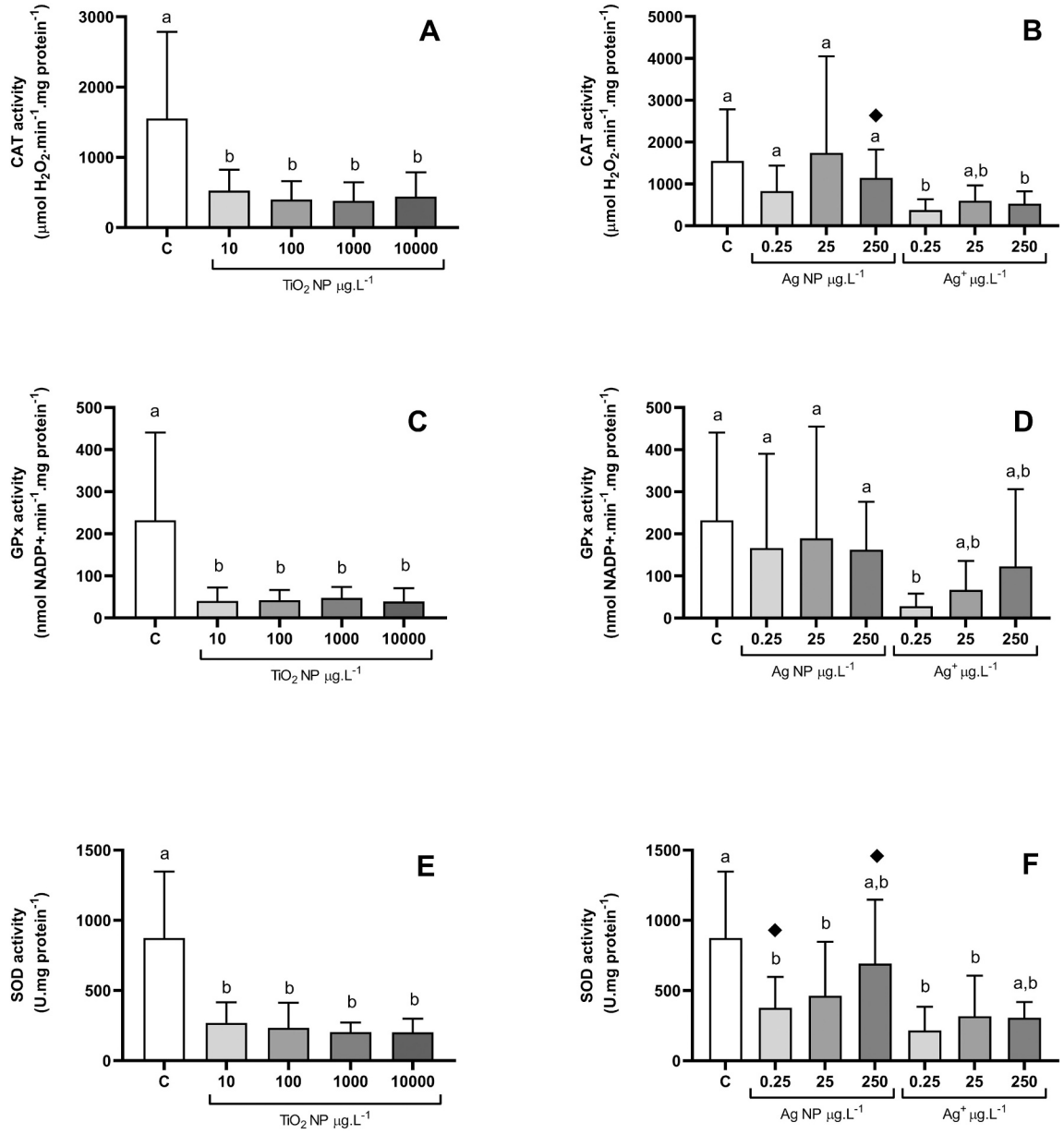

Fig. 6. Antioxidant responses in spermatozoa of *S. aurata* exposed for 1 h to (A) titanium dioxide nanoparticles (TiO_2 NP: 10, 100, 1000 and 10,000 µg·L^{-1}), as well as (B) silver nanoparticles (Ag NP: 0.25, 25 and 250 µg·L^{-1}) and silver as $AgNO_3$ ([Ag^+]: 0.25, 25 and 250 µg·L^{-1}). Different lower-case letters denote significant differences ($p < 0.05$) in relation to control. Significant differences between the corresponding concentrations of Ag NP and Ag^+ is depicted by (◆) ($p < 0.05$). Columns correspond to mean values and error bars represent the standard deviation.

4.4. *Inference for the sperm-shield effects*

The direct exposure of NP on fish sperm occurs in semen (seminal plasma and spermatozoa) and utilizes quiescent sperm. Seminal plasma protects spermatozoa from oxidative damage and thus may have functioned as a shield against NP oxidative potential (Kowalski and Cejko, 2019).

Another identified inference is related to the NP characteristics such as charge, size, coating, and concentration. NP-specific features affect their ability to induce toxicity and access the cells (Cameron et al., 2018). Lankoff et al. (2012) found that the agglomeration state affects NP's cellular localization and toxicity. These authors found that the smaller the agglomerates size, the greater its toxicity, pointing to higher toxicity of Ag NP than TiO2 NP. However, the small agglomerate size for Ag NP (235–691 nm *vs.* 131–230 nm, for TiO2 NP and Ag NP, respectively) did not reflect higher toxicity, as most of the effects occurred after TiO2 NP exposure.

The lower Ag NP toxicity may also be related to the sodium citrate coating. This coating stabilizes the NP and limits its ability to agglomerate. It also reduces the dissolution of Ag NP into Ag ion, which is generally considered more toxic (Fahmy et al., 2019).

5. Conclusions

Our study reports the effects of TiO*2* NP and Ag NP on *Sparus aurata* sperm through a multiparameter approach. The results showed no alteration in sperm TM (except for the supra environmental concentration of Ag NP), VCL, morphometry, mitochondrial function, and DNA integrity. However, TiO_2 NP induced a decrease in all the antioxidants for all concentrations and Ag NP induced SOD depletion at the lowest and intermediate concentrations. Nevertheless, this antioxidant depletion had no impact on the sperm performance. Although the *ex vivo*

exposure of *S. aurata* sperm to NP was performed with quiescent cells, this is a suitable approach to simulate the sperm post-release process. Our findings indicate a low vulnerability of *S. aurata* sperm to these NP, translated into absence or low risk after release to the marine environment, with no evidence of relevant ecological impacts. Nevertheless, further studies are required to identify *in vivo* long-term effects of these NP on the reproductive processes of marine species and their mechanism of action.

CRediT authorship contribution statement

A. Carvalhais: Formal analysis, Investigation, Data curation, Writing – original draft, Visualization. **I.B. Oliveira:** Formal analysis, Investigation, Data curation, Writing – original draft. **H. Oliveira:** Investigation. **C.C.V. Oliveira:** Investigation. **L. Ferrão:** Investigation. **E. Cabrita:** Methodology, Investigation. **J.F. Asturiano:** Methodology, Investigation. **S. Guilherme:** Investigation. **M. Pacheco:** Conceptualization, Methodology, Validation, Resources, Writing – review & editing. **C.L. Mieiro:** Conceptualization, Methodology, Validation, Investigation, Resources, Data curation, Writing – review & editing, Visualization, Supervision, Project administration, Funding acquisition.

Declaration of competing interest

The authors declare that they have no known competing financial interests or personal relationships that could have appeared to influence the work reported in this paper.

Acknowledgements

Funding: This work was supported by the Portuguese Foundation for Science and Technology (FCT, I.P.) [A. Carvalhais – SFRH/2020/05105/BD, C. Mieiro - DL57/2016, S. Guilherme - DL57/2016, C.C.V. Oliveira - DL57/2016/CP1361/CT0007, I.B. Oliveira - CEECIND/01368/2018, L. Ferrão – CCMAR/BI/0007/2019, CESAM Strategic Project - UIDP/50017/2020+UIDB/50017/2020+LA/P/0094/2020), CCMAR Strategic Project - UIDB/04326/2022]; and the Operational Program Competiveness and Internationalization, Regional Operational Program of Lisboa and Regional Operational Program of Algarve, in its FEDER/FNR component, and the Foundation for Science and Technology, in its State Budget component (OE) [project NanoReproTox - PTDC/CTA-AMB/30908/2017].

Appendix A. Supplementary data

Supplementary data to this article can be found online at https://doi.org/10.1016/j.marpolbul.2022.113487.

References

Alavi, S.M.H., Cosson, J., Bondarenko, O., Linhart, O., 2019. Theriogenology sperm motility in fishes: (III) diversity of regulatory signals from membrane to the axoneme. Theriogenology 136, 143–165. https://doi.org/10.1016/j.theriogenology.2019.06.038.

Athar, M., Iqbal, M., 1998. Ferric nitrilotriacetate promotes N-diethylnitrosamine-induced renal tumorigenesis in the rat: implications for the involvement of oxidative stress. Carcinogenesis 19, 1133–1139.

Auguste, M., Lasa, A., Pallavicini, A., Gualdi, S., Vezzulli, L., Canesi, L., 2019. Exposure to TiO 2 nanoparticles induces shifts in the microbiota composition of Mytilus galloprovincialis hemolymph. Sci. Total Environ. 670, 129–137. https://doi.org/10.1016/j.scitotenv.2019.03.133.

Azqueta, A., Gutzkow, K.B., Brunborg, G., Collins, A.R., 2011. Towards a more reliable comet assay; optimising agarose concentration, unwinding time and electrophoresis conditions. Mutat. Res. 724, 41–45. https://doi.org/10.1016/j.mrgentox.2011.05.010.

Barkalina, N., Charalambous, C., Jones, C., Coward, K., 2014. Nanotechnology in reproductive medicine: emerging applications of nanomaterials. Nanomedicine 10 (5), e921–e938. https://doi.org/10.1016/j.nano.2014.01.001.

Barmo, C., Ciacci, C., Canonico, B., Fabbri, R., Cortese, K., Balbi, T., Marcomini, A., Pojana, G., Gallo, G., Canesi, L., 2013. In vivo effects of n-TiO 2 on digestive gland and immune function of the marine bivalve Mytilus galloprovincialis. Aquat. Toxicol. 132–133, 9–18. https://doi.org/10.1016/j.aquatox.2013.01.014.

Bedlovičová, Zdenka, Strapáč, Imrich, Baláž, Matej, Salayová, Aneta, 2020. A brief overview on antioxidant activity determination of silver nanoparticles. Molecules 25 (14), 3191. https://doi.org/10.3390/molecules25143191.

Beirão, J., Zilli, L., Vilella, S., Cabrita, E., Fernández-Díez, C., Schiavone, R., Herráez, M. P., 2012a. Fatty acid composition of the head membrane and flagella affects Sparus aurata sperm quality. J. Appl. Ichthyol. 28 (6), 1017–1019. https://doi.org/10.1095/biolreprod.108.068296.

Beirão, J., Zilli, L., Vilella, S., Cabrita, E., Schiavone, R., Herráez, M.P., 2012b. Improving sperm cryopreservation with antifreeze proteins: effect on gilthead seabream (Sparus aurata) plasma membrane lipids. Biol. Reprod. 86 (2), 1–9. https://doi.org/10.1095/biolreprod.111.093401.

Billard, R., Cosson, M., 1990. The energetics of fish motility. In: Gagnon, C. (Ed.), Control of Sperm Motility: Biological and Clinical Aspects. CRC Press, pp. 153–173.

Bradford, M.M., 1976. A rapid and sensitive method for the quantitation microgram quantities of protein utilizing the principle of protein-dye binding. Anal. Biochem. 254, 248–254.

Cabrita, E., Robles, V., Cuñado, S., Wallace, J.C., Sarasquete, C., Herráez, M.P., 2005. In: Evaluation of Gilthead Sea Bream, Sparus aurata, Sperm Quality After Cryopreservation in 5ml Macrotubes, 50, pp. 273–284. https://doi.org/10.1016/j.cryobiol.2005.02.005.

Cabrita, E., Martínez-Páramo, S., Gavaia, P.J., Riesco, M.F., Valcarce, D.G., Sarasquete, C., Herráez, M.P., Robles, V., 2014. Factors enhancing fish sperm quality and emerging tools for sperm analysis. Aquaculture 432, 389–401. https://doi.org/10.1016/j.aquaculture.2014.04.034.

Cameron, S.J., Hosseinian, F., Willmore, W.G., 2018. A current overview of the biological and cellular effects of nanosilver. Int. J. Mol. Sci. 19 (7), 1–40. https://doi.org/10.3390/ijms19072030.

Canesi, L., Fabbri, R., Gallo, G., Vallotto, D., Marcomini, A., Pojana, G., 2010. Biomarkers in Mytilus galloprovincialis exposed to suspensions of selected nanoparticles (Nano carbon black, C60 fullerene, Nano-TiO 2, Nano-SiO 2). Aquat. Toxicol. 100 (2), 168–177. https://doi.org/10.1016/j.aquatox.2010.04.009.

Christen, R., Gatti, J.-L., Billard, R., 1987. Trout sperm motility: the transient movement of trout sperm is related to changes in the concentration of ATP following the activation of the flagellar movement. Eur. J. Biochem. 166 (3), 667–671. https://doi.org/10.1111/j.1432-1033.1987.tb13565.x.

Claiborne, A., 1985. Catalase activity. In: Greenwald, R.A. (Ed.), Handbook of Methods in Oxygen Radical Research, 1985. CRC Press, Boca Raton, FL, USA, pp. 283–284.

Collins, A.R., 2004. The comet assay for DNA damage and repair: principles, applications, and limitations. Appl. Biochem. Biotechnol. B Mol. Biotechnol. 26 (3), 249–261. https://doi.org/10.1385/MB:26:3:249.

Cosson, J., 2019. Fish sperm physiology: structure, factors regulating motility, and motility evaluation. In: Bozkurt, Y. (Ed.), Biological Research in Aquatic Science. IntechOpen, pp. 1–26.

Costantini, D., Rowe, M., Butler, M.W., McGraw, K.J., 2010. From molecules to living systems: historical and contemporary issues in oxidative stress and antioxidant ecology. Funct. Ecol. 24 (5), 950–959. https://doi.org/10.1111/j.1365-2435.2010.01746.x.

de Brito, J.L.M., de Lima, V.N., Ansa, D.O., Moya, S.E., Morais, P.C., de Azevedo, R.B., Lucci, C.M., 2020. Acute reproductive toxicology after intratesticular injection of silver nanoparticles (AgNPs) in Wistar rats. Nanotoxicology 14 (7), 893–907. https://doi.org/10.1080/17435390.2020.1774812.

De Jong, W.H., Hagens, W.I., Krystek, P., Burger, M.C., Sips, A.J.A.M., Geertsma, R.E., 2008. Particle size-dependent organ distribution of gold nanoparticles after intravenous administration. Biomaterials 29 (12), 1912–1919. https://doi.org/10.1016/j.biomaterials.2007.12.037.

De Lamirande, E., Jiang, H., Zini, A., Kodama, H., Gagnon, C., 1997. Reactive oxygen species and sperm physiology. Rev. Reprod. 2 (1), 48–54. https://doi.org/10.1530/ror.0.0020048.

Deycard, V.N., Schäfer, J., Petit, J.C.J., Coynel, A., Lanceleur, L., Dutruch, L., et al., 2017. Chemosphere 167 (C), 501–511. https://doi.org/10.1016/j.chemosphere.2016.09.154.

Drokin, S.I., 1993. Phospholipids and fatty acids of phospholipids of sperm from several freshwater and marine species of fish. Comp. Biochem. Physiol. 104B (2), 423–428.

Engel, K.M., Dzyuba, V., Ninhaus-silveira, A., Veríssimo-silveira, R., Dannenberger, D., Schiller, J., Steinbach, C., Dzyuba, B., 2020. Sperm lipid composition in early diverged fish species: internal vs. external mode of fertilization. Biomolecules 10 (2), 1–25. https://doi.org/10.3390/biom10020172.

Erraud, A., Bonnard, M., Duflot, A., Geffard, A., 2017. Assessment of sperm quality in palaemonid prawns using Comet assay: methodological optimization. Environ. Sci. Pollut. Res. 25 (12), 11226–11237. https://doi.org/10.1007/s11356-017-8754-6.

Fahmy, H.M., Mosleh, A.M., Elghany, A.A., Shams-Eldin, E., Abu Serea, E.S., Ali, S.A., Shalan, A.E., 2019. Coated silver nanoparticles: synthesis, cytotoxicity, and optical properties. RSC Adv. 9 (35), 20118–20136. https://doi.org/10.1039/c9ra02907a.

Falchi, L., Bogliolo, L., Galleri, G., Ariu, F., Zedda, M.T., Pinna, A., Malfatti, L., Innocenzi, P., Ledda, S., 2016. Cerium dioxide nanoparticles did not alter the functional and morphologic characteristics of ram sperm during short-term exposure. Theriogenology 85 (7), 1274–1281.e3. https://doi.org/10.1016/j.theriogenology.2015.12.011.

Gallego, V., Asturiano, J.F., 2018. Sperm motility in fish: technical applications and perspectives through CASA-Mot systems. Reprod. Fertil. Dev. 30 (6), 820–832. https://doi.org/10.1071/RD17460.

Gallego, V., Asturiano, J.F., 2019. Fish sperm motility assessment as a tool for aquaculture research, a historical approach. Rev. Aquac. 11, 697–724. https://doi.org/10.1111/raq.12253.

Gallego, V., Pérez, L., Asturiano, J.F., Yoshida, M., 2014. Sperm motility parameters and spermatozoa morphometric characterization in marine species: a study of swimmer and sessile species. Theriogenology 82 (5), 668–676. https://doi.org/10.1016/j.theriogenology.2014.05.026.

Gallo, A., Tosti, E., 2020. In: Reproductive Processes of Marine Animals as Biomarker for Environmental Stress Impact, pp. 1–16.

Gallo, A., Boni, R., Buttino, I., Tosti, E., 2016. Spermiotoxicity of nickel nanoparticles in the marine invertebrate Ciona intestinalis (ascidians). Nanotoxicology 10 (8), 1096–1104. https://doi.org/10.1080/17435390.2016.1177743.

Gallo, A., Manfra, L., Boni, R., Rotini, A., Migliore, L., Tosti, E., 2018. Cytotoxicity and genotoxicity of CuO nanoparticles in sea urchin spermatozoa through oxidative stress. Environ. Int. 118 (May), 325–333. https://doi.org/10.1016/j.envint.2018.05.034.

Gallo, A., Boni, R., Tosti, E., 2020. Gamete quality in a miltistressor environment. Environ. Int. 138, 105627 https://doi.org/10.1016/j.envint.2020.105627.

Giri, U., Iqbal, M., Athar, M., 1996. Porphyrine-mediated photosensitization has a weak tumor promoting activity in mouse skin: possible role of in situ generated reactive oxygen species. Carcinogenesis 17 (9), 2023–2028.

Griffitt, R.J., Hyndman, K., Denslow, N.D., Barber, D.S., 2009. Comparison of molecular and histological changes in zebrafish gills exposed to metallic nanoparticles. Toxicol. Sci. 107 (2), 404–415. https://doi.org/10.1093/toxsci/kfn256.

Guilherme, S., Santos, M.A., Gaivão, I., Pacheco, M., 2014. Genotoxicity evaluation of the herbicide Garlon V and its active ingredient (triclopyr) in fish (Anguilla anguilla L.) using the comet assay. Environ. Toxicol. (March), 1073–1081 doi:10.1002/tox.

Han, Y., Shi, W., Rong, J., Zha, S., Guan, X., Sun, H., Liu, G., 2019. Exposure to waterborne nTiO2 reduces fertilization success and increases polyspermy in a bivalve mollusc: a threat to population recruitment. Environ. Sci. Technol. 53 (21), 12754–12763. https://doi.org/10.1021/acs.est.9b03675.

Handy, R.D., Al-Bairuty, G., Al-Jubory, A., Ramsden, C.S., Boyle, D., Shaw, B.J., Henry, T.B., 2011. Effects of manufactured nanomaterials on fishes: a target organ and body systems physiology approach. J. Fish Biol. 79 (4), 821–853. https://doi.org/10.1080/10934520701792779.

Hook, S.E., Gallagher, E.P., Batley, G.E., 2014. The role of biomarkers in the assessment of aquatic ecosystem health. Integr. Environ. Assess. Manag. 10 (3), 327–341. https://doi.org/10.1002/ieam.1530.

Islam, M.S., Akhter, T., 2012. Tale of fish sperm and factors affecting sperm motility: a review. Adv. Life Sci. 1 (1), 11–19. https://doi.org/10.5923/j.als.20110101.03.

Keller, A.A., McFerran, S., Lazareva, A., Suh, S., 2013. Global life cycle releases of engineered nanomaterials. J. Nanopart. Res. 15 (6) https://doi.org/10.1007/s11051-013-1692-4.

Keshari, A.K., Srivastava, R., Singh, P., Yadav, V.B., Nath, G., 2020. J. Ayurveda Integr. Med. 11 (1), 37–44. https://doi.org/10.1016/j.jaim.2017.11.003.

Kowalska-Góralska, M., Dziewulska, K., Kulasza, M., 2019. Effect of copper nanoparticles and ions on spermatozoa motility of sea trout (Salmo trutta m. Trutta L.). Aquat. Toxicol. 211 (August 2018), 11–17. https://doi.org/10.1016/j.aquatox.2019.03.013.

Kowalski, R.K., Cejko, B.I., 2019. Sperm quality in fish: determinants and affecting factors. Theriogenology 135, 94–108. https://doi.org/10.1016/j.theriogenology.2019.06.009.

Kurwadkar, S., Pugh, K., Gupta, A., Ingole, S., 2015. Nanoparticles in the environment: occurrence, distribution, and risks. J. Hazard. Toxic Radioact. Waste 19 (3), 04014039. https://doi.org/10.1061/(asce)hz.2153-5515.0000258.

Labbé, C., Loir, M., 1991. Plasma membrane of trout spermatozoa: I. Isolation and partial characterization. Fish Physiol. Biochem. 9 (4), 325–338. https://doi.org/10.1007/BF02265153.

Labille, J., Slomberg, D., Catalano, R., Robert, S., Apers-Tremelo, M.-L., Boudenne, J.-L., et al., 2020. Sci. Total Environ. 706 (C), 136010. https://doi.org/10.1016/j.scitotenv.2019.136010.

Lan, Z., Yang, W.X., 2012. Nanoparticles and spermatogenesis: how do nanoparticles affect spermatogenesis and penetrate the blood-testis barrier. Nanomedicine 7 (4), 579–596. https://doi.org/10.2217/nnm.12.20.

Lankoff, A., Sandberg, W.J., Wegierek-Ciuk, A., Lisowska, H., Refsnes, M., Sartowska, B., Schwarze, P.E., Meczynska-Wielgosz, S., Wojewodzka, M., Kruszewski, M., 2012. The effect of agglomeration state of silver and titanium dioxide nanoparticles on cellular response of Hep G2, A549 and THP-1 cells. Toxicol. Lett. 208 (3), 197–213. https://doi.org/10.1016/j.toxlet.2011.11.006.

Lodeiro, P., Browning, T.J., Achterberg, E.P., Guillou, A., El-Shahawi, M.S., 2017. Mechanisms of silver nanoparticle toxicity to the coastal marine diatom Chaetoceros curvisetus. Sci. Rep. 7 (1), 1–10. https://doi.org/10.1038/s41598-017-11402-x.

Magesky, A., Pelletier, É., 2018. Cytotoxicity and physiological effects of silver nanoparticles on marine invertebrates. Adv. Exp. Med. Biol. 1048 (February), 285–309. https://doi.org/10.1007/978-3-319-72041-8_17.

Marco-Jiménez, F., Peñaranda, D.S., Pérez, L., Viudes-De-Castro, M.P., Mylonas, C.C., Jover, M., Asturiano, J.F., 2008. Morphometric characterization of sharpsnout sea bream (Diplodus puntazzo) and gilthead sea bream (Sparus aurata) spermatozoa using computer-assisted spermatozoa analysis (ASMA). J. Appl. Ichthyol. 24 (4), 382–385. https://doi.org/10.1111/j.1439-0426.2008.01135.x.

Marques, A., Marçal, R., Pereira, V., Pereira, P., Mieiro, C., Guilherme, S., et al., 2019. In: Macroalgae-enriched Diet Protects Gilthead Seabream (Sparus aurata) Against Erythrocyte Population Instability and Chromosomal Damage Induced by Aqua-medicines, pp. 1–17. https://doi.org/10.1007/s10811-019-01996-2.

Mieiro, C.L., Martins, M., Silva, M., Coelho, J.P., Lopes, C.B., Alves, A., Alves, J., Pereira, E., Pardal, M., Costa, M.H., Pacheco, M., 2019. Advances on assessing nanotoxicity in marine fish – the pros and cons of combining an ex vivo approach and histopathological analysis in gills. Aquat. Toxicol. 217 (September), 105322 https://doi.org/10.1016/j.aquatox.2019.105322.

Mohandas, J., Marshall, J., Duggins, G., Horvath, J., Tiller, D., 1984. Differential distribution of glutathione and glutathione related enzymes in rabbit kidney. Possible implications in analgesic neuropathy. Cancer Res. 44, 5086–5091.

Moretti, E., Terzuoli, G., Renieri, T., Iacoponi, F., Castellini, C., Giordano, C., Collodel, G., 2013. In vitro effect of gold and silver nanoparticles on human spermatozoa. Andrologia 45 (6), 392–396. https://doi.org/10.1111/and.12028 doi: 10.1016/j.aquaculture.2016.04.021.

Nielsen, R., Ankamah-Yeboah, I., Llorente, I., 2021. Technical efficiency and environmental impact of seabream and seabass farms. Aquac. Econ. Manag. 25 (1), 106–125. https://doi.org/10.1080/13657305.2020.1840662.

Ogunsuyi, O.M., Ogunsuyi, O.I., Akanni, O., Alabi, O.A., Alimba, C.G., Adaramoye, O.A., Cambier, S., Eswara, S., Gutleb, A.C., Bakare, A.A., 2020. Alteration of sperm parameters and reproductive hormones in Swiss mice via oxidative stress after co-exposure to titanium dioxide and zinc oxide nanoparticles. Andrologia 52 (10), 1–17. https://doi.org/10.1111/and.13758.

Oliveira, H., Spanò, M., Santos, C., Pereira, M.D.L., 2008. Lead chloride affects sperm motility and acrosome reaction in mice: lead affects mice sperm motility and acrosome reaction. Cell Biol. Toxicol. 25 (4), 341–353. https://doi.org/10.1007/s10565-008-9088-4.

Olugbodi, J.O., David, O., Oketa, E.N., Lawal, B., Okoli, B.J., Mtunzi, F., 2020. Silver nanoparticles stimulates spermatogenesis impairments and hematological alterations in testis and epididymis of male rats. Molecules 25 (5). https://doi.org/10.3390/molecules25051063.

Özgür, M.E., Balcıoğlu, S., Ulu, A., Özcan, İ., Okumuş, F., Köytepe, S., Ateş, B., 2018a. The in vitro toxicity analysis of titanium dioxide (TiO2) nanoparticles on kinematics and biochemical quality of rainbow trout sperm cells. Environ. Toxicol. Pharmacol. 62 (June), 11–19. https://doi.org/10.1016/j.etap.2018.06.002.

Özgür, M.E., Ulu, A., Balcioğlu, S., Özcan, I., Köytepe, S., Ateş, B., 2018b. The toxicity assessment of iron oxide (Fe3O4) nanoparticles on physical and biochemical quality of rainbow trout spermatozoon. Toxics 6 (4). https://doi.org/10.3390/toxics6040062.

Özgür, M.E., Ulu, A., Balcioğlu, S., Özcan, I., Okumuş, F., Köytepe, S., Ateş, B., 2018c. Investigation of toxicity properties of flower-like ZnO nanoparticles on Cyprinus carpio sperm cells using computer-assisted sperm analysis (CASA). Turk. J. Fish. Aquat. Sci. 18, 771–780. https://doi.org/10.4194/1303-2712-v18.

Özgür, M.E., Ulu, A., Özcan, İ., Balcioglu, S., Ateş, B., Köytepe, S., 2019. Investigation of toxic effects of amorphous SiO2 nanoparticles on motility and oxidative stress markers in rainbow trout sperm cells. Environ. Sci. Pollut. Res. 26 (15), 15641–15652. https://doi.org/10.1007/s11356-019-04941-5.

Özgür, M.E., Ulu, A., Noma, S.A.A., Özcan, İ., Balcıoğlu, S., Ateş, B., Köytepe, S., 2020. Melatonin protects sperm cells of Capoeta trutta from toxicity of titanium dioxide nanoparticles. Environ. Sci. Pollut. Res. 27, 17843–17853.

Rajeswari, V.D., Eed, E.M., Elfasakhany, A., et al., 2021. Green synthesis of titanium dioxide nanoparticles using Laurus nobilis (bay leaf): antioxidant and antimicrobial activities. Appl. Nanosci. https://doi.org/10.1007/s13204-021-02065-2.

Santonastaso, M., Mottola, F., Colacurci, N., Iovine, C., Pacifico, S., Cammarota, M., Cesaroni, F., Rocco, L., 2019. In vitro genotoxic effects of titanium dioxide nanoparticles (n-TiO2) in human sperm cells. Mol. Reprod. Dev. 86 (10), 1369–1377. https://doi.org/10.1002/mrd.23134.

Santonastaso, M., Mottola, F., Iovine, C., Cesaroni, F., Colacurci, N., Rocco, L., 2020. In vitro effects of titanium dioxide nanoparticles (TiO2NPs) on cadmium chloride (CdCl2) genotoxicity in human sperm cells. Nanomaterials 10 (6), 1–16. https://doi.org/10.3390/nano10061118.

Shaalan, M., Saleh, M., El-Mahdy, M., El-Matbouli, M., 2016. Recent progress in applications of nanoparticles in fish medicine: a review. Nanomedicine 12 (3), 701–710. https://doi.org/10.1016/j.nano.2015.11.005.

Shamsi, M.B., Imam, S.N., Dada, R., 2011. Sperm DNA integrity assays: diagnostic and prognostic challenges and implications in management of infertility. J. Assist. Reprod. Genet. 28 (11), 1073–1085. https://doi.org/10.1007/s10815-011-9631-8.

Shehata, A.M., Salem, F.M.S., El-Saied, E.M., Abd El-Rahman, S.S., Mahmoud, M.Y., Noshy, P.A., 2021. Zinc nanoparticles ameliorate the reproductive toxicity induced by silver nanoparticles in male rats. Int. J. Nanomedicine 16, 2555–2568. https://doi.org/10.2147/IJN.S307189.

Słowińska, M., Nynca, J., Cejko, B.I., Dietrich, M.A., Horváth, Á., Urbányi, B., Kotrik, L., Ciereszko, A., 2013. Total antioxidant capacity of fish seminal plasma. Aquaculture 400–401, 101–104. https://doi.org/10.1016/j.aquaculture.2013.03.010.

Taylor, U., Barchanski, A., Petersen, S., Kues, W.A., Baulain, U., Gamrad, L., Sajti, L., Barcikowski, S., Rath, D., 2014. Gold nanoparticles interfere with sperm functionality by membrane adsorption without penetration. Nanotoxicology 8 (Suppl. 1), 118–127. https://doi.org/10.3109/17435390.2013.859321.

Taylor, U., Tiedemann, D., Rehbock, C., Kues, W.A., Barcikowski, S., Rath, D., 2015. Influence of gold, silver and gold-silver alloy nanoparticles on germ cell function and embryo development. Beilstein J. Nanotechnol. 6 (1), 651–664. https://doi.org/10.3762/bjnano.6.66.

Van Look, K.J.W., Kime, D.E., 2003. Automated sperm morphology analysis in fishes: the effect of mercury on goldfish sperm. J. Fish Biol. 63 (4), 1020–1033. https://doi.org/10.1046/j.1095-8649.2003.00226.x.

Vignardi, C.P., Hasue, F.M., Sartório, P.V., Cardoso, C.M., Machado, A.S.D., Passos, M.J. A.C.R., Santos, T.C.A., Nucci, J.M., Hewer, T.L.R., Watanabe, I.S., Gomes, V., Phan, N.V., 2015. Genotoxicity, potential cytotoxicity and cell uptake of titanium dioxide nanoparticles in the marine fish Trachinotus carolinus (Linnaeus, 1766). Aquat. Toxicol. 158 (November), 218–229. https://doi.org/10.1016/j.aquatox.2014.11.008.

Wang, E., Huang, Y., Du, Q., Sun, Y., 2017. Silver nanoparticle induced toxicity to human sperm by increasing ROS (reactive oxygen species) production and DNA damage.

Environ. Toxicol. Pharmacol. 52 (November 2016), 193–199. https://doi.org/10.1016/j.etap.2017.04.010.

Wassall, S.R., Stillwell, W., 2009. Polyunsaturated fatty acid – cholesterol interactions: domain formation in membranes. Biochim. Biophys. Acta Biomembr. 1788 (1), 24–32. https://doi.org/10.1016/j.bbamem.2008.10.011.

Zhang, C., Hu, Z., Deng, B., 2016. Silver nanoparticles in aquatic environments: physiochemical behavior and antimicrobial mechanisms. Water Res. 88, 403–427. https://doi.org/10.1016/j.watres.2015.10.025.

Zilli, L., Schiavone, R., Storelli, C., Vilella, S., 2008. Mechanisms Determining Sperm Motility Initiation in Two Sparids (Sparus aurata and Lithognathus mormyrus). Biology of Reproduction 79 (2), 356–366. https://doi.org/10.1095/biolreprod.108.068296.

Zilli, L., Schiavone, R., Vilella, S., 2017. Role of protein phosphorilation/dephosphorylation in fish sperm motility activation: State of the art and perspectives. Aquaculture 472, 73–80. https://doi.org/10.1016/j.aquaculture.2016.03.043.